J. Santiago
H. Bernhoff

J. Electrical Systems 6-2 (2010): x-xx

Regular paper

Comparison between axial and radial flux PM coreless machines for flywheel energy storage

The need of a deeper understanding of coreless machines arises with new magnetic materials with higher remanent magnetization and the spread of high speed motors and generators. High energy density magnets allow complete ironless stator motor/generators configurations which are suitable for high speed machines and specifically in flywheel energy storage. Axial-flux and radial-flux machines are investigated and compared. The limits and merits of ironless machines are presented.

An analytic solution of Maxwell's equations is used to calculate the properties of axial-flux and radial-flux ironless generators. This method is used to investigate the influence of several parameters such as diameter and airgap width. Two machines have been calculated with FEM techniques and results are compared to validate the analytic method.

Simulations conclude that end winding effects are more significant for axial-flux than for radial-flux topologies. Radial-flux machines are more suitable for high speed ironless stators. The optimum values of some machine parameters are significantly different for ironless machines in comparison to slotted and slotless machines, such as outer radius to inner radius for axial-flux topologies. High speed coreless machines for energy storage and other applications required 3D FEM analysis for accurate results.

Keywords: Flux density, High-speed PM electric machine, Magnetic devices, Optimum design, Permanent Magnets Synchronous Machine (PMSM).

1. Introduction

Energy storage in the form of rotational kinetic energy has been use for centuries since the potter's wheel, but it was not until the 1960's and 1970's when NASA sponsored several projects that state the bases of modern fast flywheels as a reliable and efficient energy storage system [1]. The amount of energy stored in a rotational rigid body is proportional to the moment of inertia and to the square of its angular velocity. It is calculated by means of the equation

$$E = \frac{1}{2} \cdot I \cdot \omega^2 \tag{1}$$

The design strategy to obtain high energy density in flywheels is to increase the angular velocity of the flywheel, as suggested by equation (1) [2]. Modern flywheels are made of high strength composite materials to overcome centrifugal forces and achieve design speeds over 100,000 rpm. The motor/generator that drives the flywheel in energy storage systems required extreme properties such as high speed and high efficiency over a great range of variable speed. Unconventional geometric solutions such permanent magnets machines with coreless stators have been proposed [3], and motivate this comparison of coreless topologies.

The development of high energy density and high coercivity new magnetic materials has increased the design possibilities of permanent magnet motors. High energy density magnets allow an increase of the airgap without a reduction in the magnetic field density in

Corresponding author: J. Santiago
Division for Electricity, Dep. of Eng. Sciences, Uppsala University, Sweden.
juan.santiago@ angstrom.uu.se,

the airgap. This has lead to an increase of interest in slotless permant magnet synchronous motor for high performance applications .The slotless configurations has some very interesting properties as compared to traditional cored machines such:

- No cogging torque
- No teeth losses and hence a significant reduction in core losses
- Linear current – torque relation
- Lower stator inductance typically 1/10 to 1/100
- Near perfect sinusoidal back emf possible.
- No iron saturation in stator teeth

The draw back is that more permanent magnet material is needed to obtain the same magnetic field density in the airgap. All this properties lead to a potential higher efficiency than regular slotted machines [4].

The next step in the design concept of reducing the iron losses is to study the complete ironless configuration. In slotless or toothless machines, the winding is held by a ferromagnetic matrix while in ironless machines the windings are held in a non magnetic resin matrix that completely eliminate the iron losses. The benefits of completely irolnless core motors are similar to the toothless motors but increased. The absence of iron losses may be significant for high speed motors with high frequencies involved or when the idle losses are important such as in flywheel energy storage applications.

PM slotless motors are commercially available for specific applications due to their superior properties for certain applications. The average flux density in the airgap reported by [5] is 0.18 T while typical values for a commercial motor are 0.8 T in the airgap. The magnetic field in the airgap is slotted machines is limited by the steel saturation in the teeth which is about 1.8 T. If the permanent magnet technology continues to evolve, coreless machines may be designed with much higher magnetic flux density than slotted machines as they are not limited by the iron saturation. Today most promising technology has a theoretical maximum energy product (BH) of 1.5 MA/m (120 MGOe), three times higher than commercial permanent magnets. Furthermore, new materials are currently being studied [6].

Axial-flux machine are wining relevance and substituting traditional radial-flux machines in some niches of application [7]. Previous authors [8, 9, 10] have compared axial-flux and radial-flux permanent magnet brushless motor topologies, and slotted and slotless stators, with similar conclusions. Axial-flux machines can achieve higher efficiencies. This topology is more appropriated for machines with high number of poles, short axial length and low speed. Slotless machines require more copper material due to the lower magnetic flux density in the airgap.

2. Geometry bases of comparison

The geometries considered for this comparison are radial-flux and axial-flux ironless machines. In the axial-flux geometry, the stator is placed between to rotor discs with magnets [11]. The magnetic path goes from one disc to the other through the ironless stator and the return path goes through the rotating back yoke of the rotor. In this configuration there is not a single ferromagnetic element under a variable magnetic field. To achieve an analog flux path in a radial-flux configuration a hollow shape rotor is needed. The radial flux ironless motor consists of an external rotor with an inner par of the rotor that closes the magnetic field path. The stator has an empty cylinder shape and it is placed in the middle of the rotor. It can only be attached to the frame by one side. Both geometries are shown as shown in figure 1.

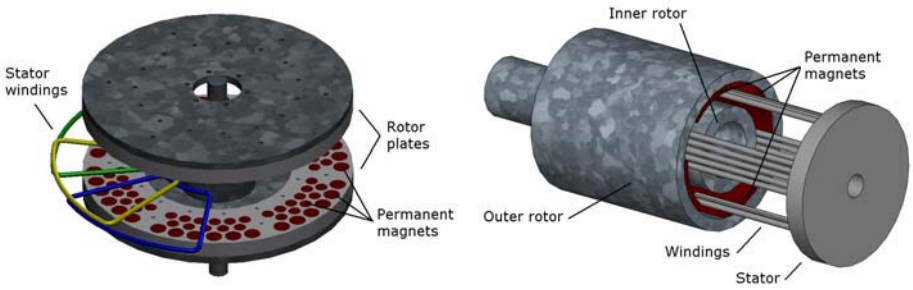

Figure 1. Ironless axial flux and radial flux machine schemes.

2.1. Mechanics

Electric motors and generators are generally constrained by mechanical or thermal limitations. As the main purpose of ironless motors is high speed applications, the mechanical limitation is studied while no thermal considerations are taken into account in this comparison. The weakest mechanical part of ironless machines is the back yoke in the rotor. To make the comparison useful, main design parameters of both types of machines have to be analog. Machines with the same rotational speed and same mechanical stress may be compared, but this restriction implies that the radii of radial and axial flux machine are different. Under these conditions, the axial flux machines have larger radii than radial flux machines.

The back yoke of an axial flux machine may be approximated to a plate while the radial flux back yoke may be approximated to an annular ring. We can analytically obtain the maximum diameter at a certain rotational speed making the stress equal to the yield strength of the material. The analytic equation for a disc is [12]:

$$\sigma_\theta = \frac{3+\nu}{8} \cdot \rho \cdot \omega^2 \cdot r_e^2 \tag{2}$$

and for an annular ring with constant thickness:

$$\sigma_\theta = \frac{3+\nu}{8} \cdot \rho \cdot \omega^2 \cdot (r_e^2 + \frac{1-\nu}{3-\nu} \cdot r_i^2) \tag{3}$$

Where σ_θ is the stress in the hoop direction at the center of the plate or at the minimum radius. Both are proportional to the density (ρ), the Poisson's ratio (ν) and the square of the rotational speed (ω) and internal and external radius (r_i and r_e). These are the points where the stress is maximum and designed to be stood by materials yield strength.

Equations (2) and (3) prove that a rotating plate with a hole in the middle stands lower speeds than the primitive disk. In other words, this property gives axial flux geometries a geometrical advantage over radial flux ones as their back yoke has a more plated shape in comparison with radial flux machines' annular ring shape. But this result is not considered in this paper as it is negligible in comparison with the effect of the centrifugal forces of the magnets against the annular ring in the radial flux geometry.

In the case of the radial flux machine, the centrifugal forces of the magnets against the yoke reduce the maximum size. The relation between magnet thickness and back yoke thickness is kept at 1.2; this value ensures high magnetization without reaching the

saturation region of the magnetic material for a four pole machine. The magnet width to the pole width is 0.7 for both configurations, so the centrifugal forces of the magnets increases the strain in the radial flux rotor by a factor of

$$K_m = 1 + \frac{\rho_{magnet}}{\rho_{iron}} \cdot \frac{h_{magnet}}{h_{iron}} \cdot \frac{\tau_{magnet}}{\tau_{pole}} = \frac{6000}{7800} \cdot \frac{1}{1.2} \cdot \frac{0.7}{1} = 1.45 \quad (4)$$

The maximum speed is proportional to the square root of the centrifugal force. Therefore relation between the maximum radii of the two geometries is:

$$\frac{\omega_r^2}{\omega_a^2} = \frac{K_m \cdot Y}{Y} \quad (5)$$

where Y is the yield strength of the back yoke. The radial flux machine is $1/\sqrt{K_m}$ times slower than the axial flux geometry. This is, about 82%.

2.2. Windings

There are several important differences in the stator topology of ironless machines in comparison with slotted machines where the windings are placed organized in the slots. Non magnetic materials such as epoxi resin or composite materials which hold the stator have lower stiffness than laminated steel.

The space for the windings is limited as it increases the airgap and higher airgaps reduce the magnetic flux density and require more magnetic material. The epoxi matrix, all the conductors and eventually a plate to hold the stator structure is confined as tight as possible. The machine presented in [5] requires a 40mm or higher airgap, which is ten times higher than equivalent slotted machines. The thickness of the magnets is proportional to the airgap and thicker magnets lead to more expensive and heavier machines and potential vibration problems. Windings in slotted machines are limited by the iron saturation and design load angle, while slottless windings are a compromise of magnet and airgap thickness, and optimization of the space in the airgap.

Traditional machines may have concentrated windings or distributed windings, represented in figure 2. In slotted machines this decision mainly depends on the amount of harmonics that the machine specifications required, but in the case of ironless machines it is a matter of packing factor. The magnetic flux distribution in large airgaps tends to be sinusoidal and concentrated windings have lower packing factors but they are mechanically simpler and easier to manufacture and therefore they are sometimes preferred like in [5]. The comparison presented in this paper considers distributed windings.

In the axial-flux configuration the concentrated winding may be embedded in a resin matrix and does not need a tray to hold the stator, but nevertheless the package factor is still very low. For axial-flux configurations the packaging in the outer part of the stator is lower than in the inner part. Radial-flux machines have some advantages in the winding distribution. The airgap area is constant in the axial direction increasing the packaging factor and the active length is higher than in axial configuration, reducing the number of end turnings.

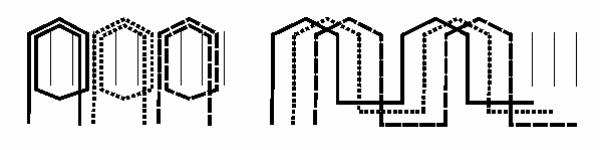

Figure 2. Sketch of concentrate winding and a distributed winding topology.

2.3. Magnetic flux configuration

In the radial-flux machine, magnets are placed in the periphery where the radius is higher. The speed at which magnets pass over the conductors in the stator is higher in the axial flux configuration than in the radial flux and therefore induces higher back electro magnetic force (emf). From the magnetic field point of view, the axial-flux configuration is superior to the radial-flux configuration, but there is an important mechanical restriction for high speed machines that should be taken into account. The strength of magnetic materials is lower than steel. If no attention is paid, the mechanical limiting point may be found in the magnets and not in the steel. To avoid cracks to appear at high speed, permanent magnets dimension should be limited. The size of the magnets is limited by Hertz formulas. The thickness of the magnets in the radial-flux topology is not limiting as the centrifugal forces acting the thickness direction are not critical. But the size of the magnets for axial flux geometries is limited for high speed machines. To reduce the stress in the magnets, poles are split into several small magnets embedded in a high resistance non ferromagnetic structure such duraluminum as seen in figure 1 [13]. The magnets can not therefore cover the whole surface of the poles and are restricted at about 60% of it.

The main issue of the magnetic flux configuration on machines with high airgaps is the end effects. In motors with an airgap 10 times larger than conventional slotted machines, end winding leakage field is no longer negligible. Figure 3 shows the magnetic field in a stator of an axial-flux machine with two rotors and an airgap of 30 mm computed in the middle of the pole. The rotor has an outer diameter of 160 mm and inner diameter of 110 mm. The active magnetic region of the rotor is 50 mm and the airgap is 30 mm, that is, in the same order of magnitude. The magnetic field that is dispersed out of the magnetic region is underlined. A quarter of the magnetic field does not remain under the magnets and the coils should cover at least 50% more area to trap 90% of the magnetic flux. The stator should cover a wither region as for slotted machines, in the range of half of the airgap at bode sides. In long radial fluxes this is not a significant change, but in axial flux has two important implications. An increase in the outer radius implies much longer end turning and shorter inner radius implies less space for windings.

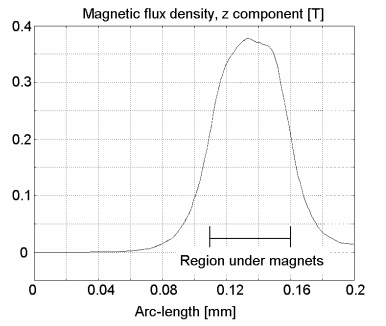

Figure 3. Magnetic field density along the radius for a radial flux machine in the middle of the airgap. Lines shows the max/min radius of the magnets.

3. Comparison procedure

The comparison of a radial-flux and an axial-flux machine presented as been done via analytic equations that have been validated through a 3D-FEM model and through the construction and measurements of a prototype machine. The machine topology and main parameters are shown in figure 4. The parameters that will vary in the study are speed of the machine, voltage and power, while the other parameters will change in relation with the variable ones. The parameters that will be kept constant are magnet thickness, airgap and current density.

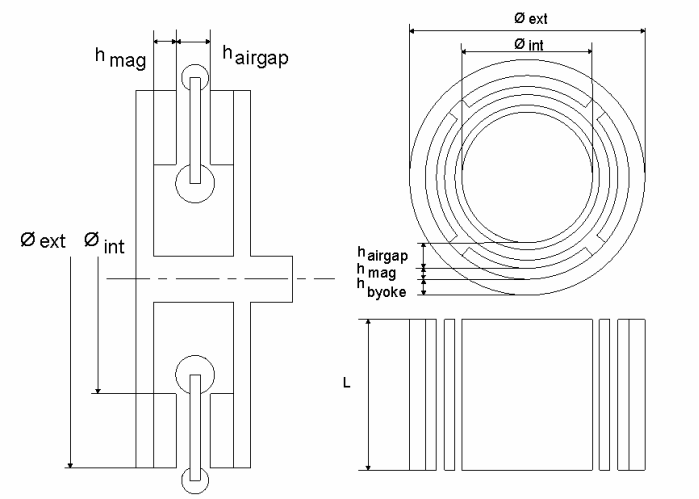

Figure 4. Schemes and main parameters of an axial-flux and a radial-flux ironless machines.

The radius of the motor is the maximum possible for the speed. The mechanical limit will be the iron back yoke according to equation (3). The radial-flux machine will be 82% of the axial-flux machine as in equation (4). The relation between speed and radius is:

$$Scale\_factor = R_{ext} / rpm = 2 \cdot 10^{-5} m / rpm \tag{6}$$

The remanent flux density B_r of the magnets is 1.2T. The area of poles covered by magnets in the axial-flux configuration is 60% as explained in the magnetic flux configuration section. The magnetic field in the airgap is estimated in a first approximation by the magnetic circuit equations. For the axial-flux geometry the magnetic field can be calculated as

$$B = 0.6 \cdot \frac{2h}{2h + g} B_r \tag{7}$$

Where h is the height of the magnet and g is the height of the airgap. The factor 0.6 is due to the fact that only 60% of the pole is covered by magnets. The magnetic field for the radial-flux configuration is calculated with an analog method. K_d is 0.95 for both configurations and the distance from the windings to the magnets is 5 mm also for both configurations.

The effective part of the airgap that is covered with copper windings is kept constant. It is fixed at 15% for both configurations to make a fair comparison thought radial flux machines are easier to wind and more compact. This value includes a plate to hold the stator with about the same thickness as the windings. The current is limited to 6 amps per

square mm. The conductor section is obtained considering the number of poles, number of turns per pole and the effective area. The end turn estimated is slightly higher than the arc length to connect successive conductor treads. The length of the conductor is obtained with the active part of the conductors plus the end winding.

The back emf is obtained with the straight application of Faraday's law as in [14]:

$$E = K_d \cdot n_p \cdot n_t \cdot l \cdot B \cdot r_{av} \cdot (rpm \cdot \frac{2 \cdot \pi}{60}) \tag{8}$$

Where n_p is the number of pole pairs, n_t the number of turns in the coils, l is the active conductor length, and r_{av} is the average distance from the conductor to the rotational axis.

4. Results analysis

4.1. Outer to inner radius in axial flux machines

The optimal ratio of outer radius to the inner radius (K_r) for axial-flux machines varies from different authors but it is generally accepted being $1/\sqrt{3}$ [9]. This thumb ruse has been revised and it has been observed that the optimal value for ironless machines is slightly higher. There is a trade off; the higher the relation the more active winding we have, but the lower package factor because there is less space in the inner part of the machine. This relation is valid for slotted machines. The influence of K_r is shown in figure 5. The maximum power that can be extracted from a generator occurs for a K_r of 0.63 when large end windings are taking into account. This value in not general and has to be obtained for every specific geometry. The electrical efficiency (considering only copper and eddy current losses and not taking into account the bearing and drag losses) is also studied. The efficiency drops for high K_r but stays quite invariable at around 0.63 as seen in figure 6.

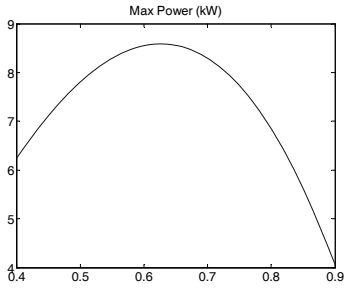

Figure 5. Power of an axial flux machine depending on the relation between inner and outer radius

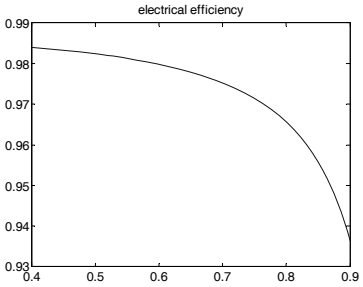

Figure 6. Efficiency of an axial-flux machine depending on the relation between inner and outer radius.

4.2. Influence of speed

When the speed increases the radius of the machine has to be smaller to overcome centrifugal forces. The number of poles and turns in the windings are constant. The back emf, efficiency, area of conductors in the airgap and maximum power extracted for an axial flux geometry are shown in figure 7. The results for a radial-flux geometry are shown in figure 8.

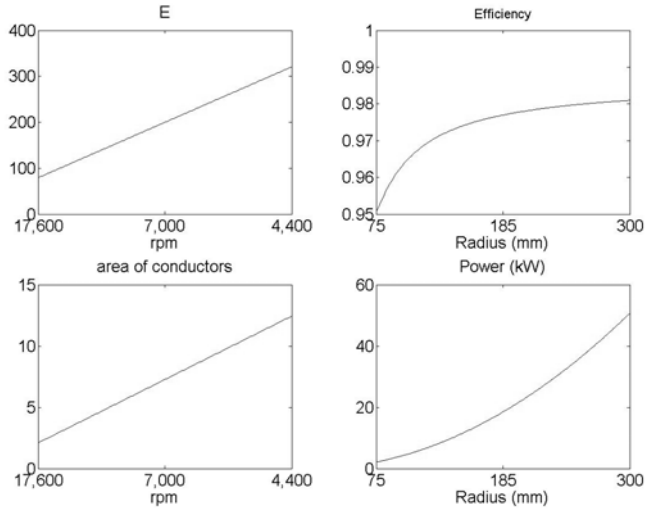

Figure 7. Relation between different parameters when the speed changes for an axial-flux topology. The speed and size change together with a scale factor. The back emf (E), efficiency and the area available for conductors increase with the radius, obtaining higher rated power.

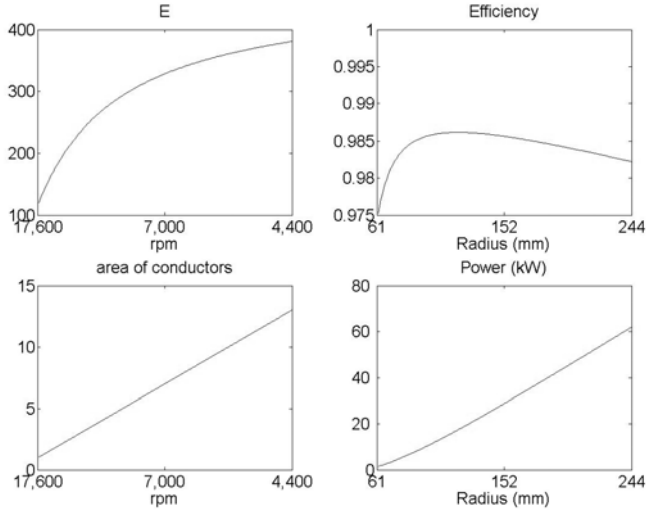

Figure 8. Relation between different parameters when the speed changes for a radial-flux topology. The speed and size change together with a scale factor.

4.3. Influence of the airgap

For a fixed speed of 10,000 rpm and magnet thickness, the influence of the airgap size is studied. Smaller airgaps produce higher magnetic flux in the airgap but allow less space for windings, reducing the area of the conductors and increasing the losses. In this comparison the area of the conductors is constant while the number of turns in the windings compensates the reduction of the airgap. Results are shown in figures 9 and 10.

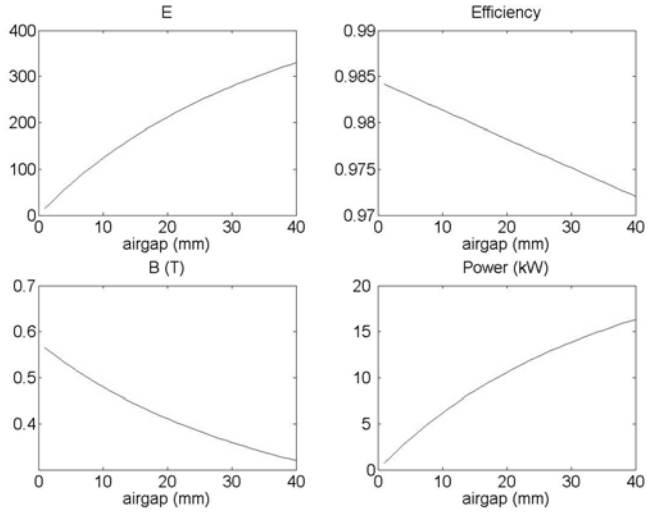

Figure 9. Axial-flux topology machine behavior when the winding thickness is increase from 1mm to 40mm.

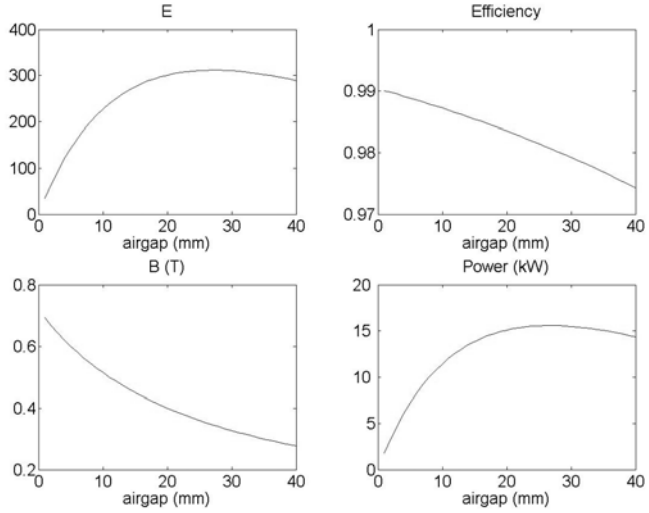

Figure 10. Radial-flux topology machine behavior when the winding thickness is increase from 1mm to 40mm.

The transversal area of the windings is proportional to the airgap in the axial-flux topology while it is proportional to the square of the airgap in radial-flux machines. The results shows that the axial-flux machine topology is more efficient and more suitable for

higher sizes and lower speeds while the radial-flux topology has better performance for high speed applications. Because of the high speed topology, only 60% of the poles in the axial-flux machine are covered with magnets. Even with this reduction in the magnetic flux, the axial-flux machine shows better performance for very low axial flux, but for high airgap sizes the radial flux topology is more efficient and has higher power rates.

4.4. Power density.

The magnetic flux density in ironless generators has lower values than traditional slotted equivalent machines, which require more magnetic material and wider active areas. Previous comparative studies between slotted and slotless machines showed this effect, and full ironless are not an exception. The recommended magnetic field in slotted machines decrease with the frequency machines [15]. For high speed machines up to 400Hz the energy density in the airgap equals the values calculated in this comparison, but the mass of magnets is about 3 times higher for slotless machines. For higher speeds, the energy density in the airgap may be higher in slotless machines. If the remanent magnetic flux of the magnets continues to increase, the extra magnetic material required in slotless machines will not represent a significant increase in weight.

5. FEM verification of the model

An axial-flux and a radial-flux machine have been simulated with a 3D FEM analysis as a comparison example. The schematic views are shown in figure 11. Main parameters of both machines are consistent with the restrictions described in previous sections.

Table I: parameters of the machines

	Axial flux	Radial flux
rpm	10,000 rpm	10,000 rpm
B_r	1.2 T	1.2 T
r_{ext} (for the same σ_θ)	132 mm	108 mm
r average (stator)	106 mm	62.5 mm
Airgap	25 mm	25 mm
Turns x poles	72	72
Magnet thickness	20 mm	15 mm
Rotor length	n.a.	135 mm
r_e/r_i	0.6	n.a.

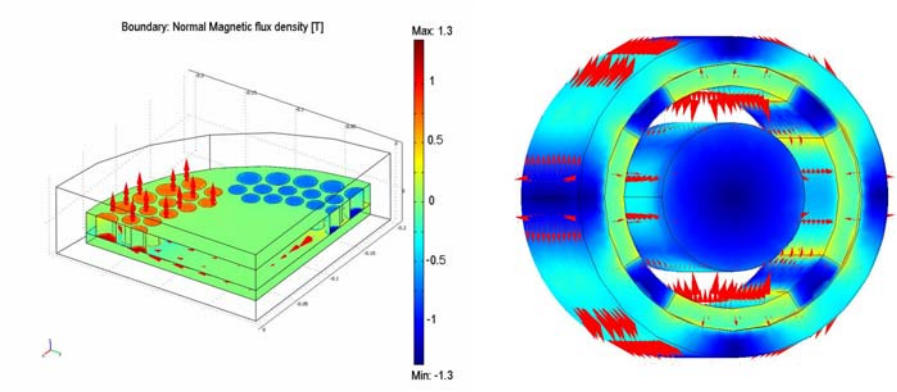

Figure 11: Magnetic flux density paths 3D FEM simulation for the axial flux and radial flux machines studied.

Due to the geometrical differences, the magnetic field dispersion is lower in the axial flux machine. This geometry has a longer active magnetic pole and the end winding effect is less pronounced. Table II shows a comparison of main machine parameters. The discrepancies between analytic and FEM methods are in the range of 6%. This discrepancy validates analytic results for qualitative studies but suggests the need of more complex calculation methods for quantitative solutions. The comparison between this two calculation methods emphasizes that end effects are more pronounced in coreless machines than in slotted machines and 3D FEM calculations are needed for detailed machine description.

Table II: FEM simulation result

	Axial Flux		Radial Flux	
	Analytic	FEM	Analytic	FEM
Max magnetic flux	0.44	0.42	0.45	0.42
Back EMF	221	215	270.4	253.7
Cable length per phase	24 m		21 m	
Conductor area	5.17 mm^2		4.07 mm^2	

The back EMF of the radial flux machine is about 25% higher for the same number of conductors in the stator. The axial flux machine has more space in the airgap to place thicker conductors, but for the same conductor area and for the same back EMF the axial flux machine needs about 30 m of cable in the windings. That is about 40% more copper in the stator.

6. Prototype results

An axial-flux 8,000 rpm machine has been constructed [16]. The stator has been winded with isolated multi stranded cables as shown in figure 12. Higher package factors may be achieved with Litz wire cables as less isolation is used. Cables have been use because their higher mechanical properties and the capability of higher voltages. Some interesting lessons have been extracted after constructing the stator. With this topology the stator requires a plate to hold the windings. The end windings are as long as calculated and presented in table II and 24 m of cable per phase were required. The stator was mounted on a glass fiber plate. This arrangement was preferred because an epoxi matrix would have been more

complex to build and less stiff. The cables require higher curvature radius than litz wires. This issue is more problematic in Axial flux machines than in Radial flux machines.

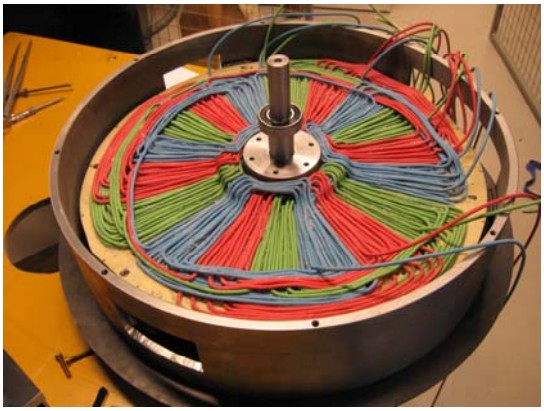

Figure 12. View of the stator of the three phase axial flux prototype.

7. Conclusion

New magnetic materials with high energy density allow slotless machines to be competitive. A study of the next design step, complete ironless machines, has been presented. Ironless configurations are especially suitable for high speed machines for flywheel energy storage and for a wide range of different applications. This paper discusses the most suitable geometries for such type of machines. Axial-flux and radial-flux ironless geometries have been compared analytically. The model has been validated with 3D FEM analysis and a prototype has been built.

Radial-flux geometries are more suitable for high speed ironless machines as the end turning effect is less significant. The stator in axial-flux machines requires high end windings, which reduces the available space, reduce the package factor more than in radial-flux geometries and increase internal resistance. The analytic study and the experience obtained after building a prototype show significant geometrical differences:

- Assumptions and thumb rules for traditional machines are not valid for ironless machines, such as the relation between inner and outer radius in axial-flux machines.
- Radial-flux has simpler and less end winding.
- Radial-flux machines are suitable for less poles which is an advantage for high speed machines.
- Axial-flux machines can achieve less magnetic material density for the same magnet width due to centrifugal force distribution.
- Radial-flux machines require smaller radius than axial-flux machines.

References

[1] Haichang Liu, and Jihai Jiang, (2007), “Flywheel energy storage—An upswing technology for energy sustainability”, Energy and Buildings Volume 39, Issue 5, May 2007, Pages 599-604.

[2] Bolund, B., Bernhoff, H., and Leijon, M. (2007), “Flywheel energy and power storage systems”, Renewable and Sustainable Energy Reviews 11 (2007) 235–258.

[3] Post, R.F., Fowler, T.K., and Post, S.F., “A high-efficiency electromechanical battery”, Proceedings of the IEEE, Vol. 81, Issue: 3, Mar 1993.

[4] Todd D. Batzel, and Kwang Y. Lee, “Slotless Permanent Magnet Synchronous Motor Operation without a High Resolution Rotor Angle Sensor”, IEEE Trans. on Energy Conversion, Vol. 15, No. 4, December 2000.

[5] Swett, D. W.; Blanche, J. G. (2005), “Flywheel charging module for energy storage used in electromagnetic aircraft launch system“, IEEE Trans. on Magnetics, vol. 41, no. 1, pt.2, p 525-8.

[6] Yang C.P., Jiang Z.L., Chen X.Y., Zhou H.W., Ma C.L., Zhu J., Wang Y.Z., Hu B.P., Zhang H.W. and Shen B.G (2001), "Microstructure and magnetic properties of two-phase nanocomposite Nd9Fe85.5Nb1.0B4.5-yCy (y=0.5-4.5) magnets", Journal of Alloys and Compounds, Vol. 316, Num. 1, pp. 269-274(6).

[7] M. Chaieb, S. Tounsi, and R. Neji, "Design and optimization of axial permanent magnet machine for electric vehicle", Journal of Electrical Systems, Vol. 5, Issue 1, March 2009

[8] Akatsu, K. and Wakui, S. (2006), "A comparison between axial and radial flux PM motor by optimum design method from the required output NT characteristics", COMPEL: The International Journal for Computation and Mathematics in Electrical and Electronic Engineering, Vol. 25 No. 2, pp. 496-509.

[9] Upadhyay, P. R. and Rajagopal, K. R. (2005), "Comparison of performance of the axial-field and radial-field permanent magnet brushless direct current motors using computer aided design and finite element methods", Journal of Applied Physics, vol. 97, issue 10Q506.

[10] Sitapati, K. and Krishnan, R. (2001), "Performance comparisons of radial and axial field, permanent-magnet, brushless machines", IEEE Trans. on Industry Applications, Vol. 37, Issue 5, pages:1219 – 1226.

[11] A. Moalla, S. Tounsi, and R. Neji, "Determination of axial flux motor electric parameters by the analytic-finite elements method", Journal of Electrical Systems, Vol. 4, Issue 4, Dec. 2008.

[12] Ragab A. R and Bayoumi S. E., Engineering Solids Mechanics, Fundamentals and Applications, CRC Press LLC(1999)

[13] Sakai, K., Tabuchi, Y. and Washizu, T. (1993), "Structure and characteristics of new high speed machines with two or three rotor discs", Industry Applications Society Annual Meeting, 1993., Conference Record of the 1993 IEEE.

[14] Upadhyay, P. R., Rajagopal K. R. and Singh B. P. (2004), "Design of a Compact Winding for an Axial-Flux Permanent-Magnet Brushless DC Motor Used in an Electric Two-Wheeler", IEEE Trans. on magnetics vol 40, no. 4.

[15] Huang, S., Jian Luo, Leonardi, F. and Lipo, T.A., (1998), "A General Approach to Sizing and Power Density Equations for Comparison of Electrical Machines", IEEE Trans. on Industry Applications, vol. 34, no. 1.

[16] Santiago, J., Oliveira, J., Lundin, J., Abrahanssom, J., Larsson, A., and Bernhoff, H., "Design Parameters Calculation of a Novel Driveline for Electric Vehicles", World Electric Vehicle Journal Vol. 3, 2009.